Original Article

Institution of MECHANICAL ENGINEERS

Journal of AEROSPACE ENGINEERING

Proc IMechE Part G:
J Aerospace Engineering
2015, Vol. 229(1) 119–134

DOI: 10.1177/0954410014527251
uk.sagepub.com/jaero

SAGE

Adaptive trajectory tracking control system design for hypersonic vehicles with parametric uncertainty

Zhen Liu, Xiangmin Tan, Ruyi Yuan, Guoliang Fan and Jianqiang Yi

Abstract

A new nonlinear adaptive control scheme based on the immersion and invariance theory is presented to achieve robust velocity and altitude tracking for hypersonic vehicles with parametric uncertainty. The longitudinal dynamics of the hypersonic vehicle are first decomposed into velocity, altitude/flight-path angle, and angle of attack/pitch rate subsystems. Then a non-certainty-equivalent controller based on immersion and invariance, consisting of a control module and a parameter estimator, is designed for each subsystem with all the aerodynamic parameters unknown. The main feature of this method lies in the construction of the estimator, which is a sum of a partial estimate generated from the update law and an additional nonlinear term. The new term is capable of assigning appointed stable dynamics to the parameter estimate error. Stability analysis is presented using Lyapunov theory and shows asymptotical convergence of the tracking error to zero. Representative simulations are performed. Rapid and accurate command tracking is demonstrated in these numerical simulations, which illustrate the effectiveness and robustness of the proposed approach.

Keywords

Hypersonic vehicles, adaptive control, tracking control, immersion and invariance method

Date received: 18 September 2013; accepted: 21 January 2014

Introduction

The interest in a readily accomplished and cost-effective access to space has been sustained throughout the past decades. To achieve this goal, the concepts of hypersonic flight vehicles, which can allow high-speed air transportation while offering increase in payload capacity and reduction in operation costs,[1] are widely explored. The most representative successes of this technology are NASA's X-43A and the very recent flight of the US Air Force's X-51A. Despite years of research, it is extensively recognized that more effective and reliable design methods, as well as major advances in propulsion and materials, are required for the development of a full-scale operational hypersonic vehicle (HSV).[2]

The nonlinear control problem associated with HSVs offers diverse challenges to the control engineers.[1–3] The large flight envelope and complex plant characteristics of HSVs both present significant difficulties in obtaining aerodynamic characteristics, which result in unavoidable modeling uncertainties. In addition, some other peculiarities of HSVs, such as the structural flexibility, strong couplings stemming from the integrated engine–airframe configuration, plant parameter variations, and large nonlinearities, should also be dealt with. All of these suggest it is a challenging problem for the control system design of HSVs.

Many research efforts on the control design problem are available in the literature. Linearization based on small perturbation theory is the most direct approach to deal with model nonlinearities. Several linear design methods are applied to the linearized dynamical models.[3–6] For this kind of flight control system design, a corresponding controller is regulated at each operating point, and then gain scheduling is used to combine these controllers throughout the flight envelope, which is a common practice in engineering. Unfortunately, the controller gain set is precomputed off-line and, therefore, cannot handle unpredictable changes.[7] Moreover, it is complex and time consuming to design large look-up tables for the unusual flight envelope of HSVs. Therefore, a number of nonlinear control techniques are investigated in

Institute of Automation, Chinese Academy of Sciences, Beijing, P.R. China

Corresponding author:
Xiangmin Tan, Institute of Automation, Chinese Academy of Sciences, 95 Zhongguancun East Road, Beijing 100190, P.R. China.
Email: feedbacknuaa@126.com

subsequent works. One of the most widely used techniques is the feedback linearization method.[8–12] To overcome the dependence on accurate models, which are essential in this method but usually difficult to obtain for HSVs, several variations of this method have been made. Sigthorsson et al.,[5,] Parker et al.,[10,11] and Rehman et al.[12] use linear quadratic regulator methods to enhance the control robustness, while Sun et al.[13] use finite time integral sliding mode. Also, some nonlinear adaptive control methods have been employed, such as adaptive sliding mode control,[8,14,15] fuzzy adaptive control,[16–18] and neural network control.[19,20] The key problem of incorporating feedback linearization with an adaptive outer loop is that the global stability of the closed-loop system or the convergence of the tracking error cannot be guaranteed.[21] The adaptive backstepping approach[22] is another way to handle nonlinearities, yet can give these guarantees simultaneously. Due to the cascaded structure of HSV's dynamics, many efforts have been made to develop the HSV control systems by the combination of backstepping theory and other control technologies.[20,23–26] Disturbance observer-based control method is applied to the control system design of HSVs as well.[27,28] This method considers active disturbance rejection and employs a nonlinear disturbance observer as a feedforward compensator in the controller design, which improves the robustness performance of some aspects.

Among the numerous challenges encountered in designing control systems for HSVs, the presence of uncertainties in both physical and aerodynamic parameters might be one of the most severe. This research focuses on this problem and aims to design a nonlinear adaptive control system to overcome the aerodynamic parameter uncertainties. A new method for adaptive control of nonlinear systems called immersion and invariance (I&I)[29,30] is applied here. This new method does not require knowledge of a Lyapunov function and yields stabilizing schemes relying on non-certainty-equivalent principles in adaptive control problems. Moreover, estimators based on this method allow for prescribed dynamics to be assigned to the estimate errors. More details about I&I can be found in Astolfi and Ortega[29] and Astolfi et al.[30] This approach has been used in some cases.[26,31–37] In Ji et al.,[26] an incorporation of dynamic inversion and backstepping, with parameter estimators based on the I&I theory, is applied to the HSV control problem. For stability analysis, auxiliary states from output filters and dynamic scaling factors are added to the estimator dynamics, which in turn makes the analysis tenebrous and cumbersome. Additionally, the standard adaptive backstepping has two major problems when it is applied directly to flight control. One is that the derivatives of intermediate virtual controls are tedious to calculate. The other is no constraints on the inputs and state variables are taken into account. The second one can be a crucial problem because of the aggressive flight envelope allowed for HSVs.[38] Due to the characteristics of scramjet engines, the state variables, for example, the angle of attack, must be maintained within an admissible range. However, no practical constraints on actuators and state variables have been taken into account in Ji et al.,[26] which result in extremely unreasonable deflections of the actuators in simulations. When these constraints are considered and the saturation of one actuator or virtual control happens, the desired control signal cannot be implemented and the tracking error cannot converge asymptotically. This will lead to corrupting the learning capabilities of online parameter update laws and the stability of the closed-loop system can no longer be assured. A command filtered backstepping approach for these two problems is presented in Farrell et al.[39,40] It uses command filters to calculate the derivatives of intermediate virtual controls and defines a compensated tracking error to replace the actual tracking error. This replacement ensures a stable parameter estimation process even when the saturation of one actuator or virtual control happens.

The main contribution of this paper lies in the derivation of an I&I based HSV control system using a constrained adaptive backstepping procedure. The significant difference between the proposed method and the aforementioned literature is that all the aerodynamic parameters are assumed unknown. The research focuses on the trajectory tracking control of the velocity and altitude under the presence of such uncertainties. Similar to Fiorentini et al.,[24] the design satisfactorily addresses the issue of stability robustness with respect to parameter uncertainties because the control system design is independent of these parameters. The paper is organized as follows. ''HSV model and problem formulation'' section introduces the longitudinal model of a generic HSV and presents the control objectives. The non-certainty-equivalent nonlinear adaptive control law based on I&I and command filtered backstepping is derived in ''Nonlinear adaptive control system design'' section, along with analysis of the system stability. ''Simulations'' section presents performance of the proposed adaptive control law via numerical simulations, in which the constraints on actuators and state variables are considered. Finally, conclusions are given in the final section.

HSV model and problem formulation

Ignoring the flexibility effects of the body structure and assuming a flat Earth, the longitudinal dynamics of HSV can be described by[8]

$$\dot{V} = \frac{T\cos\alpha - D}{m} - \frac{\mu\sin\gamma}{r^2}$$
$$\dot{h} = V\sin\gamma$$

$$\begin{aligned}\dot{\gamma} &= \frac{L + T\sin\alpha}{mV} - \frac{(\mu - V^2 r)\cos\gamma}{Vr^2}\\ \dot{\alpha} &= Q - \dot{\gamma}\\ \dot{Q} &= \frac{M}{I_{yy}}\end{aligned} \tag{1}$$

where V, h, γ, α, Qdenote the flight velocity, altitude, flight-path angle, angle of attack, and pitch rate, respectively; μ is the gravitational constant; and $r = h + R_E$, with R_E the radius of the earth.

The thrust T, the aerodynamic forces L, D, and the aerodynamic moment M are given by

$$\begin{aligned}L &= qSC_L\\ D &= qSC_D\\ T &= qSC_T\\ M &= qS\bar{c}C_M\end{aligned} \tag{2}$$

where q is the dynamic pressure, S the reference area, and $\bar{c}$ the reference length. The approximations of the aerodynamic coefficients are given as follows

$$\begin{aligned}C_L &= C_{L\alpha}\alpha\\ C_D &= C_{D\alpha^2}\alpha^2 + C_{D\alpha}\alpha + C_{D0}\\ C_T &= C_{T\phi}\phi + C_{T0}\\ C_M(\alpha) &= C_{M\alpha^2}\alpha^2 + C_{M\alpha}\alpha + C_{M0}\\ C_M(\delta_e) &= c_e(\delta_e - \alpha)\\ C_M(Q) &= \bar{c}Q(C_{MQ\alpha^2}\alpha^2 + C_{MQ\alpha}\alpha + C_{MQ0})/(2V)\\ C_M &= C_M(\alpha) + C_M(\delta_e) + C_M(Q)\end{aligned} \tag{3}$$

where the elevator deflection δ_e and the fuel equivalence ratio ϕ are the control inputs. It should be pointed out that a canard is used as an auxiliary input in some research.[5,24] Although it can offer some benefits in decoupling the elevator deflection to the lift force,[11,24] thus rendering the system minimum phase, the presence of the canard is debatable for the vehicle physical structure because of the huge thermal stress at hypersonic speed.[41] Additionally, the control authority of the canard is quite small, so only an elevator is available for the attitude control in the present paper. The elevator is modeled as a first-order system, with the deflection limits of $\pm 20^\circ$and rate limits of $\pm 50^\circ/s$, while the engine is modeled by a second-order system[8,24] with an amplitude interval of $[0.05, 1.5]$

$$\ddot{\phi} = -2\xi\omega_n\dot{\phi} - \omega_n^2\phi + \omega_n\phi_c \tag{4}$$

In general, there are various uncertainties in the HSV dynamics and how to handle them is one of the most important issues in the control system design. Here, all the aerodynamic coefficients in equation (3) are assumed to be unknown constant parameters. The control objective is to design a control law to achieve robust velocity and altitude tracking in the presence of parameter uncertainties. Only a cruise flight condition is discussed here. Considering the structural constraints and the operability of scramjet engines, an admissible set for the attitude of the HSV is defined as follows[24]

$$\begin{aligned}\Omega := \{&-3^\circ \leqslant \gamma \leqslant 3^\circ,\ -5^\circ \leqslant \alpha \leqslant 10^\circ,\\ &-10^\circ/s \leqslant Q \leqslant 10^\circ/s\}\end{aligned} \tag{5}$$

Nonlinear adaptive control system design

According to equation (1), the longitudinal motion of HSV can be divided into two parts, namely the velocity subsystem and the altitude subsystem.[23,24] The two parts can be controlled separately. The fuel equivalence ratio, ϕ, is used directly to control the thrust and hence velocity, while the deflection of the elevator, δ_e, is the primary effector for the attitude angle, and hence altitude. The altitude subsystem is further divided into the outer-loop (h, γ) subsystem (the altitude and flight-path angle subsystem) and the inner-loop (α, Q) subsystem (the angle of attack and pitch rate subsystem). Three I&I based adaptive controllers are designed for the velocity subsystem, the (h, γ) subsystem, and the (α, Q) subsystem, respectively. Moreover, a command filter is used to accommodate physical constraints on each actuator command or intermediate virtual control. The configuration of the whole control system is shown in Figure 1.

The idea behind the I&I method is to design a control law which guarantees that the controlled system asymptotically behaves like a target system.[29] For adaptive control problems, the design procedure of I&I based control systems can be described as follows.[33] First, find a control law using unknown parameters as known ones, such that the closed-loop system has desired dynamics, and treat the closed-loop system as the target system. Second, design an update law for the unknown parameters such that the original system will be extended into a space of vehicle states and parameter estimates. Then, add an additional term to the parameter estimates, which is judiciously chosen to render the manifold attractive and invariant. The role of this new term is to shape the manifold into which the adaptive system is immersed.[29] Finally, the augmented system will have an asymptotically stable equilibrium. The control scheme based on I&I for the velocity subsystem is shown in Figure 2.

Controller design for the velocity subsystem

Assuming the commanded velocity as V_c, the tracking error is $\tilde{V} = V - V_c$. By substituting the expressions of T, D, and C_T, C_D into the first equation of

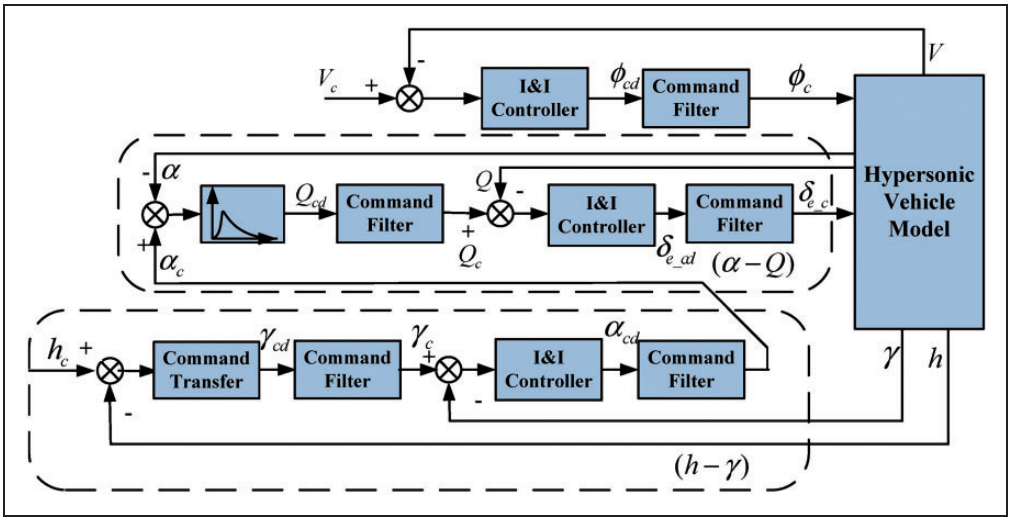

Figure 1. The configuration of the whole control system.

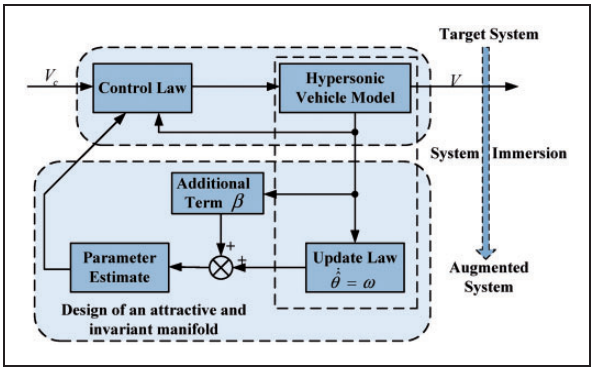

Figure 2. Graphical illustration of the I&I based controller for the velocity subsystem.

equation (1), the dynamics of the tracking error $\tilde{V}$can be written as

$$\dot{\tilde{V}} = \sigma_V\, \theta_{2V}\, \phi + \boldsymbol{\varphi}_V(\tilde{V})^T\, \boldsymbol{\theta}_{1V} - \frac{\mu \sin\gamma}{r^2} - \dot{V}_c \tag{6}$$

where

$$\boldsymbol{\varphi}_V(\tilde{V}) = \frac{qS}{m}[\cos\alpha,\ -\alpha^2,\ -\alpha,\ -1]^T$$
$$\boldsymbol{\theta}_{1V} = [C_{T0}, C_{D\alpha^2}, C_{D\alpha}, C_{D0}]^T$$
$$\theta_{2V} = C_{T\phi}$$
$$\sigma_V = \frac{qS\cos\alpha}{m}$$

$\boldsymbol{\theta}_{1V}$and $\theta_{2V}(\theta_{2V} > 0)$ are unknown parameters whose estimations are used in the controller design.

Non-certainty-equivalent control law design for the velocity subsystem. Since $\boldsymbol{\theta}_{1V}$ and θ_{2V} are not known, their estimates are needed for synthesis. In the classical adaptive control design based on the certainty equivalence (CE) philosophy, parameter estimate update laws are carefully designed by perfect cancelation of terms with uncertainty in the time derivative of Lyapunov-like function.[42] This ensures boundedness of all the resulting closed-loop signals. However, the transient performance of the estimation errors is discussed little.[30] Unlike this, the I&I approach adds to the estimate $\hat{\theta}_{iV}$ a new term, β_{iV}, the introduction of which allows construction of the error dynamic system. In other words, the estimate, $\hat{\theta}_{iV}$, generated by the update law is not applied directly in the controller, but treated as only a partial estimate, which makes the I&I approach depart from the CE philosophy.

The full estimates of the unknown parameters $\boldsymbol{\theta}_1 V$ and θ_{2V} are defined as $\hat{\boldsymbol{\theta}}_{1V} + \boldsymbol{\beta}_{1V}$ and $\hat{\theta}_{2V} + \beta_{2V}$, respectively. Then the estimate errors can be written as

$$\begin{cases} \boldsymbol{z}_{1V} = \hat{\boldsymbol{\theta}}_{1V} + \boldsymbol{\beta}_{1V} - \boldsymbol{\theta}_{1V} \\ z_{2V} = \hat{\theta}_{2V} + \beta_{2V} - \theta_{2V} \end{cases} \tag{7}$$

Select the nominal control law as

$$\phi_{cd} = [\sigma_V(\hat{\theta}_{2V} + \beta_{2V})]^{-1}\Big[-k_V\tilde{V} - \boldsymbol{\varphi}_V(\tilde{V})^T\,(\hat{\boldsymbol{\theta}}_{1V} + \boldsymbol{\beta}_{1V}) + \frac{\mu\sin\gamma}{r^2} + \dot{V}_c\Big] \tag{8}$$

where $k_V > 0$. Pass ϕ_{cd} through a command filter to generate signals ϕ_c and $\dot{\phi}_c$ within physical constraints. Therefore, ϕ_c is achievable by the actuator, and thus it can be assumed $\phi = \phi_c$. A thorough survey of the command filter is given in Farrell et al.[39,40] Define the compensated velocity tracking error as

$$\tilde{x}_V = \tilde{V} - \varepsilon_V \tag{9}$$

where according to Farrell et al.[39] ε_V can be defined as

$$\dot{\varepsilon}_V = -k_V\varepsilon_V + \sigma_V(\hat{\theta}_{2V} + \beta_{2V}(\cdot))(\phi_c - \phi_{cd}) \tag{10}$$

According to equations (9) and (10), the compensated velocity tracking error converges to the actual velocity

tracking error if the physical constraints on the engine are not in effect. Differentiating equation (9) and using equations (6), (8), and (10) gives the dynamics of the compensated tracking error

$$\dot{\tilde{x}}_V = -k_V \tilde{x}_V - \boldsymbol{\Phi}_V^T \boldsymbol{z}_V \tag{11}$$

where $\boldsymbol{z}_V = [\boldsymbol{z}_{1V}^T, z_{2V}]^T$ and $\boldsymbol{\Phi}_V = [\boldsymbol{\varphi}_V(\tilde{V})^T, \sigma_V \phi]^T$.

Note that the system in equation (11) has an asymptotically stable equilibrium at the origin when $\boldsymbol{\Phi}_V^T \boldsymbol{z}_V = 0$ and it follows that $\lim_{t\to\infty} \tilde{x}_V = 0$ from Barbalat's lemma.[43]

Parameter estimator design for the velocity subsystem. As mentioned earlier, the estimates $\hat{\theta}_{iV}$ and β_{iV} are needed in the designed control law. This section will present the design of the parameter estimator. First, differentiating equation (7) gives

$$\dot{\boldsymbol{z}}_V = \dot{\hat{\boldsymbol{\theta}}}_V + \frac{\partial \boldsymbol{\beta}_V}{\partial \tilde{x}_V} \dot{\tilde{x}}_V \tag{12}$$

where $\hat{\boldsymbol{\theta}}_V = [\hat{\boldsymbol{\theta}}_{1V}^T, \hat{\theta}_{2V}]^T$, $\boldsymbol{\beta}_V = [\boldsymbol{\beta}_{1V}^T, \beta_{2V}]^T$. Substituting equation (11) into equation (12) yields

$$\dot{\boldsymbol{z}}_V = \dot{\hat{\boldsymbol{\theta}}}_V + \frac{\partial \boldsymbol{\beta}_V}{\partial \tilde{x}_V}(-k_V \tilde{x}_V - \boldsymbol{\Phi}_V^T \boldsymbol{z}_V) \tag{13}$$

In view of equation (13), the update law is chosen as

$$\dot{\hat{\boldsymbol{\theta}}}_V = -\frac{\partial \boldsymbol{\beta}_V}{\partial \tilde{x}_V}(-k_V \tilde{x}_V) \tag{14}$$

Substituting equation (14) into equation (13) yields

$$\dot{\boldsymbol{z}}_V = -\frac{\partial \boldsymbol{\beta}_V}{\partial \tilde{x}_V} \boldsymbol{\Phi}_V^T \boldsymbol{z}_V \tag{15}$$

Note now that the nonlinear function $\boldsymbol{\beta}_V$ should be chosen to guarantee the $\boldsymbol{z}_V$ dynamics are stable. This is a huge advantage for the I&I approach over the existing ones. The extra degree of freedom in designing adaptive laws, namely the selection of $\boldsymbol{\beta}_V$, allows the construction of the $\boldsymbol{z}_V$ dynamics, which yields a significant improvement of the closed-loop performance. It is in sharp contrast with the classical nonlinear adaptive control whose dynamical behavior of the estimation errors cannot be regulated. For simplicity, choose $\boldsymbol{\beta}_V$ as

$$\frac{\partial \boldsymbol{\beta}_V}{\partial \tilde{x}_V} = \boldsymbol{r}_V \boldsymbol{\Phi}_V \tag{16}$$

where $\boldsymbol{r}_V = diag[r_{1V} \boldsymbol{I}_{4\times 4}, r_{2V}]$ and $r_{1V} > 0, r_{2V} > 0$. Substituting equation (16) into equation (15) yields

$$\dot{\boldsymbol{z}}_V = -\boldsymbol{r}_V \boldsymbol{\Phi}_V \boldsymbol{\Phi}_V^T \boldsymbol{z}_V \tag{17}$$

According to equation (16), $\boldsymbol{\beta}_V$ is obtained. Substituting it into equation (14) gives $\dot{\hat{\boldsymbol{\theta}}}_V$. Then the nominal control law ϕ_{cd} can be derived from equation (8). Passing ϕ_{cd} through the command filter shown in Farrell et al.[39] gives achievable signals ϕ_c, which is within the magnitude and rate limitations of the engine.

Stability analysis for the velocity subsystem. To begin with, recall the dynamics of $\tilde{V}$and $\boldsymbol{z}$ in equations (11) and (17)

$$\begin{cases} \dot{\tilde{x}}_V = -k_V \tilde{x}_V - \boldsymbol{\Phi}_V^T \boldsymbol{z}_V \\ \dot{\boldsymbol{z}}_V = -\boldsymbol{r}_V \boldsymbol{\Phi}_V \boldsymbol{\Phi}_V^T \boldsymbol{z}_V \end{cases} \tag{18}$$

Now consider the function $W_{2V}(\boldsymbol{z}_V) = \frac{1}{2} \boldsymbol{z}_V^T \boldsymbol{r}_V^{-1} \boldsymbol{z}_V$, whose time derivative along the trajectories of equation (18) satisfies

$$\dot{W}_{2V}(\boldsymbol{z}_V) = -(\boldsymbol{\Phi}_V^T \boldsymbol{z}_V)^2 \leqslant 0$$

which implies $\boldsymbol{z}_V(t) \in \mathcal{L}_\infty$ and $\boldsymbol{\Phi}_V^T \boldsymbol{z}_V(t) \in \mathcal{L}_2$. The first equation of equation (18) can be treated as an asymptotically stable system perturbed by a square-integrable signal. For the stability analysis of the closed-loop system, select a Lyapunov function

$$W_V(\tilde{x}_V, \boldsymbol{z}_V) = \frac{1}{2} \tilde{x}_V^2 + k_V^{-1} W_{2V}(\boldsymbol{z}_V) \tag{19}$$

Differentiating $W_V(\tilde{x}_V, \boldsymbol{z}_V)$ yields

$$\dot{W}_V(\tilde{x}_V, \boldsymbol{z}_V) = -k_V \tilde{x}_V^2 - \tilde{x}_V \boldsymbol{\Phi}_V^T \boldsymbol{z}_V - k_V^{-1} (\boldsymbol{\Phi}_V^T \boldsymbol{z}_V)^2 \tag{20}$$

By Young's inequality

$$-\tilde{x}_V \boldsymbol{\Phi}_V^T \boldsymbol{z}_V \leqslant \frac{1}{2} k_V |\tilde{x}_V|^2 + \frac{1}{2} k_V^{-1} \left| \boldsymbol{\Phi}_V^T \boldsymbol{z}_V \right|^2 \tag{21}$$

Substituting equation (21) into equation (20) yields

$$\dot{W}_V(\tilde{x}_V, \boldsymbol{z}_V) \leqslant -\frac{1}{2} k_V |\tilde{x}_V|^2 - \frac{1}{2} k_V^{-1} \left| \boldsymbol{\Phi}_V^T \boldsymbol{z}_V \right|^2 \leqslant 0 \tag{22}$$

It follows that the system in equation (18) has a globally asymptotically stable equilibrium at the origin. Furthermore, all trajectories of equation (19) converge to the invariant set $M = \{(\tilde{x}_V, \boldsymbol{z}_V) \in \boldsymbol{R} \times \boldsymbol{R}^5 : \boldsymbol{\Phi}_V^T \boldsymbol{z}_V = 0\}$. As analyzed earlier, this again demonstrates that compensated velocity tracking error asymptotically converges to zero, namely $\lim_{t\to\infty} \tilde{x}_V = 0$.

Controller design for the (h, γ) subsystem

Assuming the commanded altitude is h_c, consider the second equation of equation (1). There is no uncertainty in this equation and it is a simple but strictly

accurate bijection. Therefore, the altitude command can be accurately transformed into flight-path angle command.

Motivated by Astolfi et al.,[30] the nominal flight-path angle command is chosen as

$$\gamma_{cd} = -\arctan(k_h(h - h_c))$$

where $k_h > 0$, which yields the dynamics of the altitude

$$\dot{h} = -V\frac{k_h(h - h_c)}{\sqrt{1 + (k_h(h - h_c))^2}}$$

This confirms the dynamics of h have a globally asymptotically stable equilibrium at $h = h_c$. In other words, the altitude can track the altitude command if the flight-path angle can track the flight-path angle command.[27] Filter the nominal flight-path angle command, γ_{cd}, to produce the magnitude and rate limited command signal γ_c and its derivative $\dot{\gamma}_c$. Now $\gamma_c$is the new variable to be tracked.

To begin with, defining the tracking error as $\tilde{\gamma} = \gamma - \gamma_c$, and using the expressions of L and C_L, the dynamics of $\tilde{\gamma}$ can be written as

$$\dot{\tilde{\gamma}} = \sigma_\gamma\, \theta_{2\gamma}\, \alpha + \varphi_\gamma(\tilde{\gamma}) \tag{23}$$

where

$$\varphi_\gamma(\tilde{\gamma}) = -\frac{(\mu - V^2 r)\cos\gamma}{Vr^2} - \dot{\gamma}_c,$$
$$\theta_{2\gamma} = C_{L\alpha},\ \sigma_\gamma = qS/(mV)$$

$\theta_{2\gamma}(\theta_{2\gamma} > 0)$ is an unknown parameter. Note that the effect of the thrust T is ignored in equation (23) since the control authority of $T\sin\alpha$ is significantly smaller than that of L.

Non-certainty-equivalent control law design for the (h, γ) subsystem. Similar to the design of the I&I controller for the velocity subsystem, the full estimate of the unknown parameter $\theta_{2\gamma}$ is defined as $\hat{\theta}_{2\gamma} + \beta_{2\gamma}$, where $\beta_{2\gamma}$ is a nonlinear function to be determined and $\hat{\theta}_{2\gamma}$ is the update law.

The estimate error is

$$z_{2\gamma} = \hat{\theta}_{2\gamma} + \beta_{2\gamma} - \theta_{2\gamma} \tag{24}$$

Select the nominal virtual control signal α_{cd} as

$$\alpha_{cd} = [\sigma_\gamma(\hat{\theta}_{2\gamma} + \beta_{2\gamma})]^{-1}(-k_\gamma\tilde{\gamma} - \varphi_\gamma(\tilde{\gamma})) - \varepsilon_\alpha \tag{25}$$

where $k_\gamma > 0$ and ε_α will be defined in the next section. Pass α_{cd} through the command filter shown in Farrell et al.[39] to produce the magnitude and rate limited command signal α_c and its derivative $\dot{\alpha}_c$. Define the compensated flight-path angle tracking error as

$$\tilde{x}_\gamma = \tilde{\gamma} - \varepsilon_\gamma \tag{26}$$

where

$$\dot{\varepsilon}_\gamma = -k_\gamma\varepsilon_\gamma - \sigma_\gamma(\hat{\theta}_{2\gamma} + \beta_{2\gamma}(\cdot))(\alpha_c - \alpha_{cd}) \tag{27}$$

It can be seen that the compensated flight-path angle tracking error converges to the actual flight-path angle tracking error if the constraints on the virtual control are not in effect. Differentiating equation (26) and using equations (23), (25), and (27) gives the dynamics of $\tilde{x}_\gamma$

$$\dot{\tilde{x}}_\gamma = -k_\gamma\tilde{x}_\gamma + \sigma_\gamma(\tilde{x}_\alpha - \alpha)z_{2\gamma} + \sigma_\gamma\theta_{2\gamma}\tilde{x}_\alpha \tag{28}$$

where $\tilde{x}_\alpha$ is the compensated angle of attack tracking error that will be discussed in the next section. Note also that, according to Barbalat's lemma, the system in equation (28) has an asymptotically stable equilibrium at the origin and $\lim_{t\to\infty}\tilde{x}_\gamma = 0$ when the states converge to the set $E_\gamma = \{(\tilde{x}_\alpha, z_{2\gamma}) \in R \times R : \tilde{x}_\alpha = 0, \sigma_\gamma(\tilde{x}_\alpha - \alpha)z_{2\gamma} = 0\}$.

Parameter estimator design for the (h, γ) subsystem. Differentiating equation (24) and using equation (28) yields

$$\dot{z}_{2\gamma} = \dot{\hat{\theta}}_{2\gamma} + \frac{\partial\beta_{2\gamma}}{\partial\tilde{x}_\gamma}(-k_\gamma\tilde{x}_\gamma + \sigma_\gamma(\tilde{x}_\alpha - \alpha)z_{2\gamma} + \sigma_\gamma\theta_{2\gamma}\tilde{x}_\alpha) \tag{29}$$

Choose the update law

$$\dot{\hat{\theta}}_{2\gamma} = \frac{\partial\beta_{2\gamma}}{\partial\tilde{x}_\gamma}k_\gamma\tilde{x}_\gamma \tag{30}$$

Substituting equation (30) into equation (29) yields

$$\dot{z}_{2\gamma} = \frac{\partial\beta_{2\gamma}}{\partial\tilde{x}_\gamma}(\sigma_\gamma(\tilde{x}_\alpha - \alpha)z_{2\gamma} + \sigma_\gamma\theta_{2\gamma}\tilde{x}_\alpha) \tag{31}$$

Select now the nonlinear function $\beta_{2\gamma}$ to guarantee the $z_{2\gamma}$ dynamics have stable behavior

$$\frac{\partial\beta_{2\gamma}}{\partial\tilde{x}_\gamma} = -r_{2\gamma}\sigma_\gamma(\tilde{x}_\alpha - \alpha) \tag{32}$$

where $r_{2\gamma} > 0$. Substituting equation (32) into equation (31) yields

$$\dot{z}_{2\gamma} = -r_{2\gamma}[\sigma_\gamma(\tilde{x}_\alpha - \alpha)]^2 z_{2\gamma} - r_{2\gamma}\sigma_\gamma^2\theta_{2\gamma}(\tilde{x}_\alpha - \alpha)\tilde{x}_\alpha \tag{33}$$

$\beta_{2\gamma}$ is given from equation (32) and then $\dot{\hat{\theta}}_{2\gamma}$ is derived from equation (30). So the nominal control signal α_{cd} of equation (25) can be obtained and then the

magnitude and rate limited command signal α_c can be got from the command filter.

Stability analysis for the (h, γ) *subsystem.* Consider the Lyapunov function

$$W_\gamma(\tilde{x}_\gamma, z_{2\gamma}) = \frac{1}{2}\tilde{x}_\gamma^2 + \frac{1}{2}k_\gamma^{-1} z_{2\gamma}\, r_{2\gamma}^{-1} z_{2\gamma}$$

Its time derivative along the trajectories of equations (28) and (33) is

$$\begin{aligned}\dot{W}_\gamma(\tilde{x}_\gamma, z_{2\gamma}) &= -k_\gamma \tilde{x}_\gamma^2 + \sigma_\gamma(\tilde{x}_\alpha - \alpha) z_{2\gamma}\tilde{x}_\gamma + \sigma_\gamma \theta_{2\gamma}\tilde{x}_\alpha \tilde{x}_\gamma \\ &\quad - k_\gamma^{-1}[\sigma_\gamma(\tilde{x}_\alpha - \alpha) z_{2\gamma}]^2 \\ &\quad - k_\gamma^{-1}\sigma_\gamma^2 \theta_{2\gamma}(\tilde{x}_\alpha - \alpha)\tilde{x}_\alpha z_{2\gamma} \\ &\leqslant -\frac{1}{2}k_\gamma |\tilde{x}_\gamma|^2 - \frac{1}{2}k_\gamma^{-1}|\sigma_\gamma(\tilde{x}_\alpha - \alpha) z_{2\gamma}|^2 \\ &\quad + \sigma_\gamma \theta_{2\gamma}\tilde{x}_\alpha \tilde{x}_\gamma - k_\gamma^{-1}\sigma_\gamma^2 \theta_{2\gamma}(\tilde{x}_\alpha - \alpha)\tilde{x}_\alpha z_{2\gamma}\end{aligned} \tag{34}$$

According to equation (34), $\dot{W}_\gamma(\tilde{x}_\gamma, z_{2\gamma})$ is negative definite if $\tilde{x}_\alpha$ is zero. But $\tilde{x}_\alpha$ cannot be frozen at zero since $\tilde{x}_\alpha = \alpha - \alpha_c - \varepsilon_\alpha$ and α cannot be fixed equal to α_c. Note that the stability analysis is not yet completed. In the following section, some negative terms will be added to dominate the remaining positive terms in equation (34).

Controller design for the (α, Q) *subsystem*

The magnitude and rate limited command signal α_c is determined by the (h, γ) subsystem. Consider now the tracking error $\tilde{\alpha} = \alpha - \alpha_c$ and select the nominal command trajectory for the pitch rate as

$$Q_{cd} = -k_\alpha \tilde{\alpha} + \dot{\gamma} + \dot{\alpha}_c - \varepsilon_Q \tag{35}$$

with $k_\alpha > 0$. ε_Q will be defined in the following. Pass Q_{cd} through the command filter and then the magnitude and rate limited command signal Q_c and its derivative $\dot{Q}_c$ can be obtained. Define the compensated angle of attack tracking error as

$$\tilde{x}_\alpha = \tilde{\alpha} - \varepsilon_\alpha \tag{36}$$

where

$$\dot{\varepsilon}_\alpha = -k_\alpha \varepsilon_\alpha + Q_c - Q_{cd} \tag{37}$$

Differentiating equation (36) and using equations (35) and (37) and the fourth equation of equation (1) gives the dynamics of $\tilde{x}_\alpha$ as

$$\dot{\tilde{x}}_\alpha = -k_\alpha \tilde{x}_\alpha + \tilde{x}_Q \tag{38}$$

where $\tilde{x}_Q$ is the compensated pitch rate tracking error that will be discussed in the following. It is straightforward to show that the dynamics of $\tilde{x}_\alpha$ have a globally asymptotically stable equilibrium at the origin if $\tilde{x}_Q = 0$. Now Q_c is the new variable to be tracked. Substituting the expressions of M and $C_M(\alpha)$, $C_M(\delta_e)$, $C_M(Q)$ into the fifth equation of equation (1) yields the dynamics of $\tilde{Q}$ as

$$\dot{\tilde{Q}} = \sigma_Q\, \theta_{2Q}\, \delta_e + \boldsymbol{\varphi}_Q(\tilde{Q})^T\, \boldsymbol{\theta}_{1Q} - \dot{Q}_c \tag{39}$$

where

$$\begin{aligned}\boldsymbol{\varphi}_Q(\tilde{Q}) &= \frac{qS\bar{c}}{I_{yy}}\left[-\alpha^2, \alpha, 1, \frac{\bar{c}Q}{2V}\alpha^2, \frac{\bar{c}Q}{2V}\alpha, \frac{\bar{c}Q}{2V}\right]^T \\ \boldsymbol{\theta}_{1Q} &= [C_{M\alpha^2}, C_{M\alpha} - c_e, C_{M0}, C_{MQ\alpha^2}, C_{MQ\alpha}, C_{MQ0}]^T \\ \theta_{2Q} &= c_e \\ \sigma_Q &= \frac{qS\bar{c}}{I_{yy}}\end{aligned}$$

$\boldsymbol{\theta}_{1Q}$ and $\theta_{2Q} (\theta_{2Q} > 0)$ are unknown parameters.

Non-certainty-equivalent control law design for the (α, Q) *subsystem.* The full estimates of the unknown parameters $\boldsymbol{\theta}_{1Q}$ and θ_{2Q} are defined, respectively, as $\hat{\boldsymbol{\theta}}_{1Q} + \boldsymbol{\beta}_{1Q}$ and $\hat{\theta}_{2Q} + \beta_{2Q}$, with the estimate errors

$$\begin{cases} \boldsymbol{z}_{1Q} = \hat{\boldsymbol{\theta}}_{1Q} + \boldsymbol{\beta}_{1Q} - \boldsymbol{\theta}_{1Q} \\ z_{2Q} = \hat{\theta}_{2Q} + \beta_{2Q} - \theta_{2Q} \end{cases} \tag{40}$$

where $\boldsymbol{\beta}_{1Q}$, β_{2Q} are nonlinear functions to be determined and $\dot{\hat{\boldsymbol{\theta}}}_{1Q}$, $\dot{\hat{\theta}}_{2Q}$ are the update laws.

Select the nominal control law

$$\begin{aligned}\delta_{e\_cd} = [\sigma_Q(\hat{\theta}_{2Q} + \beta_{2Q})]^{-1}[&-k_Q\tilde{Q} + \dot{Q}_c \\ &- \boldsymbol{\varphi}_Q(\tilde{Q})^T(\hat{\boldsymbol{\theta}}_{1Q} + \boldsymbol{\beta}_{1Q}) - \tilde{x}_\alpha]\end{aligned} \tag{41}$$

where $k_Q > 0$. Filter δ_{e_cd} to produce δ_{e_c} within the magnitude and rate limitations of the actuator system. Different from the command filters for intermediate virtual controls, the filter here is first order with deflection and rate limits as described in "HSV model and problem formulation" section. Since δ_{e_c} is achievable, it can be assumed $\delta_{e\_c} = \delta_e$. Define the compensated pitch rate tracking error as

$$\tilde{x}_Q = \tilde{Q} - \varepsilon_Q \tag{42}$$

where

$$\dot{\varepsilon}_Q = -k_Q \varepsilon_Q + \sigma_Q(\hat{\theta}_{2Q} + \beta_{2Q})(\delta_{e\_c} - \delta_{e\_cd}) \tag{43}$$

Differentiating equation (42) and using equations (39), (41), and (43), the dynamics of $\tilde{x}_Q$ are

$$\dot{\tilde{x}}_Q = -k_Q \tilde{x}_Q - \boldsymbol{\Phi}_Q^T \boldsymbol{z}_Q - \tilde{x}_\alpha \tag{44}$$

where $\boldsymbol{z}_Q = [\boldsymbol{z}_{1Q}^T, z_{2Q}]^T$ and $\boldsymbol{\Phi}_Q = [\boldsymbol{\varphi}_Q(\tilde{Q})^T, \sigma_Q \delta_e]^T$.

It is apparent that the system in equation (44) has an asymptotically stable equilibrium at the origin when $\tilde{x}_\alpha = 0$ and $\boldsymbol{\Phi}_Q^T \boldsymbol{z}_Q = 0$.

Parameter estimator design for the (α, Q) subsystem. Differentiating equation (40) and using equation (44) yields

$$\dot{\boldsymbol{z}}_Q = \dot{\hat{\boldsymbol{\theta}}}_Q + \frac{\partial \boldsymbol{\beta}_Q}{\partial \tilde{x}_Q}(-k_Q \tilde{x}_Q - \boldsymbol{\Phi}_Q^T \boldsymbol{z}_Q - \tilde{x}_\alpha) \tag{45}$$

where $\hat{\boldsymbol{\theta}}_Q = [\hat{\boldsymbol{\theta}}_{1Q}^T, \hat{\theta}_{2Q}]^T$, $\boldsymbol{\beta}_Q = [\boldsymbol{\beta}_{1Q}^T, \beta_{2Q}]^T$. Select the update law as

$$\dot{\hat{\boldsymbol{\theta}}}_Q = \frac{\partial \boldsymbol{\beta}_Q}{\partial \tilde{x}_Q}(k_Q \tilde{x}_Q + \tilde{x}_\alpha) \tag{46}$$

Substituting equation (46) into equation (45) yields

$$\dot{\boldsymbol{z}}_Q = -\frac{\partial \boldsymbol{\beta}_Q}{\partial \tilde{x}_Q} \boldsymbol{\Phi}_Q^T \boldsymbol{z}_Q \tag{47}$$

Choose now the nonlinear function $\boldsymbol{\beta}_Q$ to guarantee the dynamics of $\boldsymbol{z}_Q$ have stable behavior at the origin. One choice is

$$\frac{\partial \boldsymbol{\beta}_Q}{\partial \tilde{x}_Q} = \boldsymbol{r}_Q \boldsymbol{\Phi}_Q \tag{48}$$

where $\boldsymbol{r}_Q = diag[r_{1Q} \boldsymbol{I}_{6\times 6}, r_{2Q}]$ and $r_{1Q} > 0$, $r_{2Q} > 0$. Substituting equation (48) into equation (47) yields

$$\dot{\boldsymbol{z}}_Q = -\boldsymbol{r}_Q \boldsymbol{\Phi}_Q \boldsymbol{\Phi}_Q^T \boldsymbol{z}_Q \tag{49}$$

Now $\boldsymbol{\beta}_Q$ and $\dot{\hat{\boldsymbol{\theta}}}_Q$ can be derived from equations (48) and (46) sequentially. Then the nominal control law δ_{e_cd} in equation (41) is obtained. Using a command filter again yields achievable signals δ_{e_c}, which are within the magnitude and rate limitations of the actuator system.

Stability analysis for the (α, Q) subsystem. Invoke the function $W_{2Q}(\boldsymbol{z}_Q) = \frac{1}{2} \boldsymbol{z}_Q^T \boldsymbol{r}_Q^{-1} \boldsymbol{z}_Q$, whose time derivative satisfies

$$\dot{W}_{2Q}(\boldsymbol{z}_Q) = -(\boldsymbol{\Phi}_Q^T \boldsymbol{z}_Q)^2 \leqslant 0$$

Hence $\boldsymbol{z}_Q(t) \in \mathcal{L}_\infty$ and $\boldsymbol{\Phi}_Q(t)^T \boldsymbol{z}_Q(t) \in \mathcal{L}_2$. Consider the Lyapunov function

$$W_{\alpha-Q}(\tilde{x}_\alpha, \tilde{x}_Q, \boldsymbol{z}_Q) = \frac{1}{2}\tilde{\alpha}^2 + \frac{1}{2}\tilde{Q}^2 + k_Q^{-1} W_{2Q}(\boldsymbol{z}_Q)$$

with

$$\begin{aligned} \dot{W}_{\alpha-Q}(\tilde{x}_\alpha, \tilde{x}_Q, \boldsymbol{z}_Q) &= -k_\alpha \tilde{x}_\alpha^2 + \tilde{x}_\alpha \tilde{x}_Q - k_Q \tilde{x}_Q^2 \\ &\quad - \tilde{x}_Q \boldsymbol{\Phi}_Q^T \boldsymbol{z}_Q - \tilde{x}_\alpha \tilde{x}_Q - k_Q^{-1} (\boldsymbol{\Phi}_Q^T \boldsymbol{z}_Q)^2 \\ &= -k_\alpha \tilde{x}_\alpha^2 - k_Q \tilde{x}_Q^2 - \tilde{x}_Q \boldsymbol{\Phi}_Q^T \boldsymbol{z}_Q - k_Q^{-1} (\boldsymbol{\Phi}_Q^T \boldsymbol{z}_Q)^2 \\ &\leqslant -k_\alpha |\tilde{x}_\alpha|^2 - \frac{1}{2} k_Q |\tilde{x}_Q|^2 - \frac{1}{2} k_Q^{-1} \left| \boldsymbol{\Phi}_Q^T \boldsymbol{z}_Q \right|^2 \\ &\leqslant 0 \end{aligned} \tag{50}$$

which implies $\tilde{x}_\alpha$, $\tilde{x}_Q$, and $\boldsymbol{z}_Q$ are globally asymptotically stable at the origin.

Note finally that the control laws in equations (8), (25), (35), and (41) all consist of a simple linear feedback term, such as $-k_V \tilde{V}$, and a term to cancel out the dependence on the unknown parameters, such as $\boldsymbol{\varphi}_V (\tilde{V})^T (\hat{\boldsymbol{\theta}}_{1V} + \boldsymbol{\beta}_{1V})$. The linear feedback term, with which the system perturbed by an $\mathcal{L}_2$ signal is rendered asymptotically stable as analyzed earlier, can certainly be replaced by a wide class of nonlinear feedback schemes, thus allowing dealing with more complex perturbations. Moreover, in contrast with the CE control law, additional feedback terms β_{iV}, $\beta_{i\gamma}$, β_{iQ} are employed here, which are used to construct stable dynamics of the estimate errors shown in equation (15), (31), and (47).

Stability analysis for the whole system

To examine the stability of the whole closed-loop system, we define a composite Lyapunov function

$$W = W_V(\tilde{x}_V, \boldsymbol{z}_V) + W_\gamma(\tilde{x}_\gamma, z_{2\gamma}) + \eta W_{\alpha-Q}(\tilde{x}_\alpha, \tilde{x}_Q, \boldsymbol{z}_Q)$$

with $\eta > 0$. Differentiating it and using equations (22), (34), and (50) gives

$$\begin{aligned} \dot{W} \leqslant & -\frac{1}{2} k_V |\tilde{x}_V|^2 - \frac{1}{2} k_V^{-1} \left| \boldsymbol{\Phi}_V^T \boldsymbol{z}_V \right|^2 \\ & - \frac{1}{2} k_\gamma |\tilde{x}_\gamma|^2 - \frac{1}{2} k_\gamma^{-1} |\sigma_\gamma(\tilde{x}_\alpha - \alpha) z_{2\gamma}|^2 \\ & + \sigma_\gamma \theta_{2\gamma} \tilde{x}_\alpha \tilde{x}_\gamma - k_\gamma^{-1} \sigma_\gamma^2 \theta_{2\gamma} (\tilde{x}_\alpha - \alpha) \tilde{x}_\alpha z_{2\gamma} \\ & - \eta k_\alpha |\tilde{x}_\alpha|^2 - \frac{1}{2} \eta k_Q |\tilde{x}_Q|^2 - \frac{1}{2} \eta k_Q^{-1} \left| \boldsymbol{\Phi}_Q^T \boldsymbol{z}_Q \right|^2 \\ = & -\frac{1}{2} k_V |\tilde{x}_V|^2 - \frac{1}{2} k_V^{-1} \left| \boldsymbol{\Phi}_V^T \boldsymbol{z}_V \right|^2 \\ & - \left[|\tilde{x}_\gamma|, |\sigma_\gamma(\tilde{x}_\alpha - \alpha) z_{2\gamma}|, |\tilde{x}_\alpha| \right] \mathbf{P_1} \left[|\tilde{x}_\gamma|, \right. \\ & \left. \times |\sigma_\gamma(\tilde{x}_\alpha - \alpha) z_{2\gamma}|, |\tilde{x}_\alpha| \right]^T \\ & - \frac{1}{2} \eta k_Q |\tilde{x}_Q|^2 - \frac{1}{2} \eta k_Q^{-1} \left| \boldsymbol{\Phi}_Q^T \boldsymbol{z}_Q \right|^2 \end{aligned} \tag{51}$$

where

$$\mathbf{P_1} = \begin{bmatrix} \frac{k_\gamma}{2} & 0 & -\frac{\sigma_\gamma \theta_{2\gamma}}{2} \\ 0 & \frac{1}{2k_\gamma} & \frac{\sigma_\gamma \theta_{2\gamma}}{2k_\gamma} \\ -\frac{\sigma_\gamma \theta_{2\gamma}}{2} & \frac{\sigma_\gamma \theta_{2\gamma}}{2k_\gamma} & \eta k_\alpha \end{bmatrix}$$

According to equation (51), $\dot{W}$ is negative definite if $\mathbf{P_1}$ is a positive-definite matrix. Now the existence

of the parameter η making $\mathbf{P_1}$ positive definite, thus guaranteeing the stability of the closed-loop system, is discussed. It is apparent that the first- and second-order leading principal minors of $\mathbf{P_1}$ are both positive. So $\mathbf{P_1}$ is positive definite if the determinant of $\mathbf{P_1}$ is positive. The determinant of $\mathbf{P_1}$ is

$$\begin{aligned}\det(\mathbf{P_1}) &= k_\gamma\left(k_\gamma^{-1}\eta k_\alpha - \frac{1}{4}(k_\gamma^{-1}\eta\sigma_\gamma\theta_{2\gamma})^2\right) \\ &\quad - \left(\frac{1}{2}\sigma_\gamma\theta_{2\gamma}\right)^2 k_\gamma^{-1}\eta \\ &= \left(k_\alpha - \frac{1}{4}k_\gamma^{-1}(\sigma_\gamma\theta_{2\gamma})^2\right)\eta - \frac{1}{4}k_\gamma^{-1}(\sigma_\gamma\theta_{2\gamma})^2\eta^2 \\ &= \frac{k_\gamma}{2}\left(\frac{\eta k_\alpha}{2k_\gamma} - \left(\frac{\sigma_\gamma\theta_{2\gamma}}{2k_\gamma}\right)^2\right) - \frac{\sigma_\gamma\theta_{2\gamma}}{2}\cdot\frac{\sigma_\gamma\theta_{2\gamma}}{2}\cdot\frac{1}{2k_\gamma} \\ &= \frac{\eta k_\alpha}{4} - \frac{(\sigma_\gamma\theta_{2\gamma})^2}{4k_\gamma}\end{aligned}$$

It is clear that selecting $\eta > (\sigma_\gamma\theta_{2\gamma})^2/(k_\alpha k_\gamma)$ renders $\det(\mathbf{P_1}) > 0$. Note that the value of η is only needed for the stability analysis, which is not necessary for the design of the controllers. According to equation (51), one finds $(\tilde{x}_V, \tilde{x}_\gamma, \tilde{x}_\alpha, \tilde{x}_Q, \boldsymbol{z}_V, z_{2\gamma}, \boldsymbol{z}_Q) \in \mathcal{L}_\infty$ and $(\tilde{x}_V, \tilde{x}_\gamma, \tilde{x}_\alpha, \tilde{x}_Q, \boldsymbol{\Phi}_V^T\boldsymbol{z}_V, \sigma_\gamma(\tilde{x}_\alpha - \alpha)z_{2\gamma}, \boldsymbol{\Phi}_Q^T\boldsymbol{z}_Q) \in \mathcal{L}_2$. Since $(\boldsymbol{\Phi}_V, \sigma_\gamma(\tilde{x}_\alpha - \alpha)\,, \boldsymbol{\Phi}_Q)$ and their time derivatives are bounded, it follows that $\lim_{t\to\infty}(\tilde{x}_V, \tilde{x}_\gamma, \tilde{x}_\alpha, \tilde{x}_Q, \boldsymbol{\Phi}_V^T\boldsymbol{z}_V, \sigma_\gamma(\tilde{x}_\alpha - \alpha)z_{2\gamma}, \boldsymbol{\Phi}_Q^T\boldsymbol{z}_Q) = \mathbf{0}$. It should be pointed out that the stability guarantee is for the compensated tracking errors, yet not for the actual tracking errors. When no saturation occurs, the actual tracking errors will converge to zero as the compensated tracking errors converge to zero. However, when saturation occurs, the actual tracking errors may increase while the compensated tracking errors still converge to zero. This makes the parameter estimation process stable even when the constraints are in effect, because the compensated tracking errors are used to replace the actual tracking errors in the parameter update laws.

Simulations

This section presents simulation results to verify the proposed nonlinear adaptive control system. The HSV parameters in Xu et al.[8] are used for computation. Note that the nominal aerodynamic parameters are only used in the simulation model, while their estimates are used in the control system design. The initial flying states of the HSV are chosen as $[V, h, \gamma, \alpha, Q]^T = [4590.3\,\text{m/s},\ 33,528\,\text{m},\ 0^\circ,\ 1.87^\circ,\ 0^\circ/\text{s}]^T$, while the initial control inputs are $[\delta_e, \phi]^T = [-0.55^\circ, 0.21]^T$. The actuators relative to the elevator and the engine are modeled as a first-order system with a time constant of 0.025 and a second-order system with a natural frequency of 20 rad/s and a damping factor of 0.7, respectively. The command filters for intermediate virtual controls are fixed with a natural frequency of 100 and a damping factor of 1.[37] Also, the deflection and rate limits are defined in "HSV model and problem formulation" section. The rate limits for the control signals ϕ, γ, α, and Q are not considered. The first set of simulations is performed on the nominal model. Next, parameter uncertainty is considered in the second set, where an aggressive disturbance is assumed to exist in the aerodynamic coefficients. Finally, for the purpose of comparison, the response results obtained using the incorporation of pole placement and feedback linearization[44] are presented. Two different kinds of reference trajectories for the altitude and velocity are implemented in each set of simulations. Both the altitude and velocity reference trajectories have been generated by filtering step reference commands through a second-order prefilter with a natural frequency of 0.1 rad/s and a damping factor of 0.9. In all simulations, the initial values of the estimated parameters are selected as

$$\hat{\boldsymbol{\theta}}_{1V} = 0.01ones(4),\ \hat{\theta}_{2V} = 0.001,\ \hat{\theta}_{2\gamma} = 1,$$
$$\hat{\boldsymbol{\theta}}_{1Q} = 0.01ones(6),\ \hat{\theta}_{2Q} = 0.1$$

where $ones(n) \in R^n$ denotes a vector whose elements are all 1. The control parameters are fixed as

$$[k_V, k_h, k_\gamma, k_\alpha, k_Q]^T = [1, 5\times10^{-5}, 20, 1, 0.1]^T,$$
$$[r_{1V}, r_{2V}, r_{2\gamma}, r_{1Q}, r_{2Q}]^T = [1\times10^{-4}, 1\times10^{-4}, 1, 0.01, 1]^T.$$

Simulation without parameter uncertainty

In the first set simulation study, the nominal model is used. To illustrate the performance and robustness of the proposed control law, two kinds of reference trajectories are implemented. In the first case, a step altitude and velocity command of 1000 m and 100 m/s are defined. The results of this simulation are shown in Figure 3. Figure 3(a) and (b) shows effective tracking performances for the velocity and altitude. Both the achieved velocity and altitude increase rapidly to the desired values. Figure 3(c) to (e) indicates the tracking performances of the flight-path angle γ, the angle of attack α, and the pitch rate Q relative to the virtual control inputs γ_c, α_c, and Q_c are acceptable. It can also be noted that during the whole simulation the time history of these states remains within the admissible set defined in equation (5), which is a necessary requisite for the air-breathing HSV. The deflections of the elevator δ_e and the fuel equivalence ratio ϕ are shown in Figure 3(f) and (g), both of which behave within their physical bounds. Finally, Figure 3(h) to (j) shows $\boldsymbol{\Phi}_V(\cdot)^T\boldsymbol{z}_V$, $\Phi_\gamma(\cdot)z_{2\gamma}$, and $\boldsymbol{\Phi}_Q(\cdot)^T\boldsymbol{z}_Q$ are all convergent to zero. According to the foregoing analysis, this implies the compensated tracking errors satisfy that $\lim_{t\to\infty}\tilde{x}_V = 0$, $\lim_{t\to\infty}\tilde{x}_\gamma = 0$, and $\lim_{t\to\infty}\tilde{x}_Q = 0$.

A more aggressive command is considered in the second case. The reference trajectory of the altitude

change is set as a square wave signal with an amplitude of 1000 mand a period of 150 s, while the velocity command is a step signal with an amplitude of 200 m/s. The closed-loop system tracks the command as shown in Figure 4. Figure 4(a) and (b) displays that the I&I adaptive controllers provide rapid and accurate tracking of the altitude and velocity commands, which is the control objective of the proposed controllers. Precise tracking of the commands of flight-path angle, angle of attack, and pitch rate can also be seen in Figure 4(c) to (e), respectively. Figure 4(f) and (g) shows the time history of the actuators δ_e and ϕ. The dashed-dotted line denotes the nominal command for the engine, while the solid line denotes the actual command in Figure 4(g). It can be seen that there is a short period of saturation during simulation, but the parameter estimation process remains stable because the compensated tracking errors are used to replace the actual tracking errors in the parameter update laws. Apart from the transient process at the beginning of the simulation, both δ_e and ϕ deflect periodically along with the square wave-altitude command. Note also that γ, α, and Q remain within the admissible set defined in equation (5), while δ_e and ϕ range within their physical bounds. Figure 4(h) to (j) shows that $\boldsymbol{\Phi}_V(\cdot)^T z_V$, $\Phi_\gamma(\cdot) z_{2\gamma}$, and $\boldsymbol{\Phi}_Q(\cdot)^T z_Q$ converge to zero, with small-scale oscillations when the amplitude of the square wave-altitude signal changes.

Simulation with parameter uncertainty

In the second simulation study, to illustrate the robustness of the control system to uncertainties, parameter uncertainty is considered. The form of parameter uncertainty is chosen as

$$\begin{cases} C_L = C_L^*(1 + U_{fL} + U_v) \\ C_D = C_D^*(1 + U_{fD} + U_v) \\ C_T = C_T^*(1 + U_{fT} + U_v) \\ C_M = C_M^*(1 + U_{fM} + U_v) \end{cases}$$

where C^* is the nominal value, U_f is a fixed parameter uncertainty, and U_v is a time-varying part. The uncertainties considered here are $U_{fL} = -20$ %, $U_{fD} = 20$ %, $U_{fT} = -20$ %, $U_{fM} = 20$ %, and $U_v = 0.2\sin(0.1t)$. Note that the selection of the fixed parameter uncertainty makes a 20% decrease in the lift and thrust while a 20% increase in the drag, which results in a quite aggressive situation for flight control. Moreover, the time-varying part further poses difficulty on the control laws developed here. It should also be pointed out that the maximum parameter variation considered here is up to 40% due to the complex flight characteristics of HSVs. All of these make the simulation study relatively challenging but quite representative to evaluate the robustness performance of the proposed control system to parameter uncertainty.

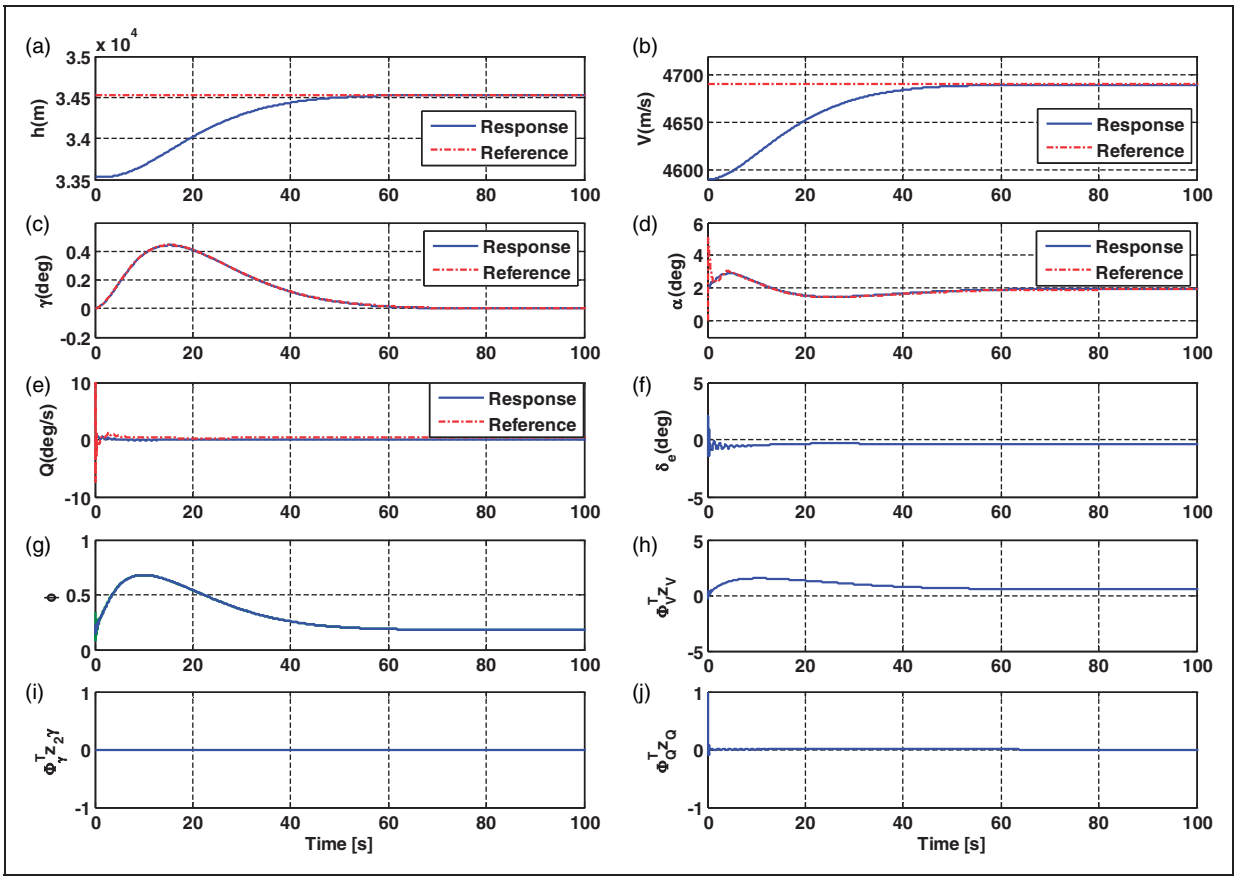

Figure 3. Responses to a 100 m/s step-velocity command and a 1000 m step-altitude command for the nominal model.

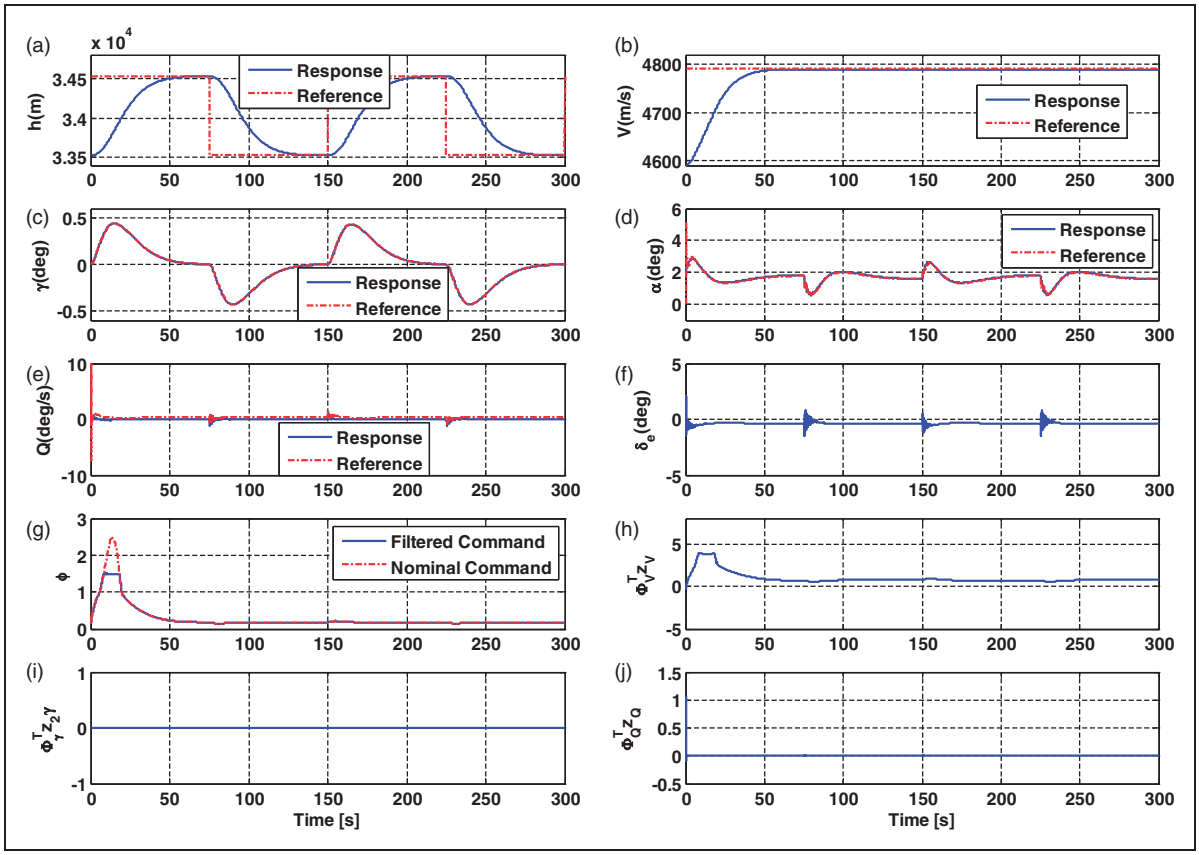

Figure 4. Responses to a 200 m/s step-velocity command and a square wave-altitude command for the nominal model.

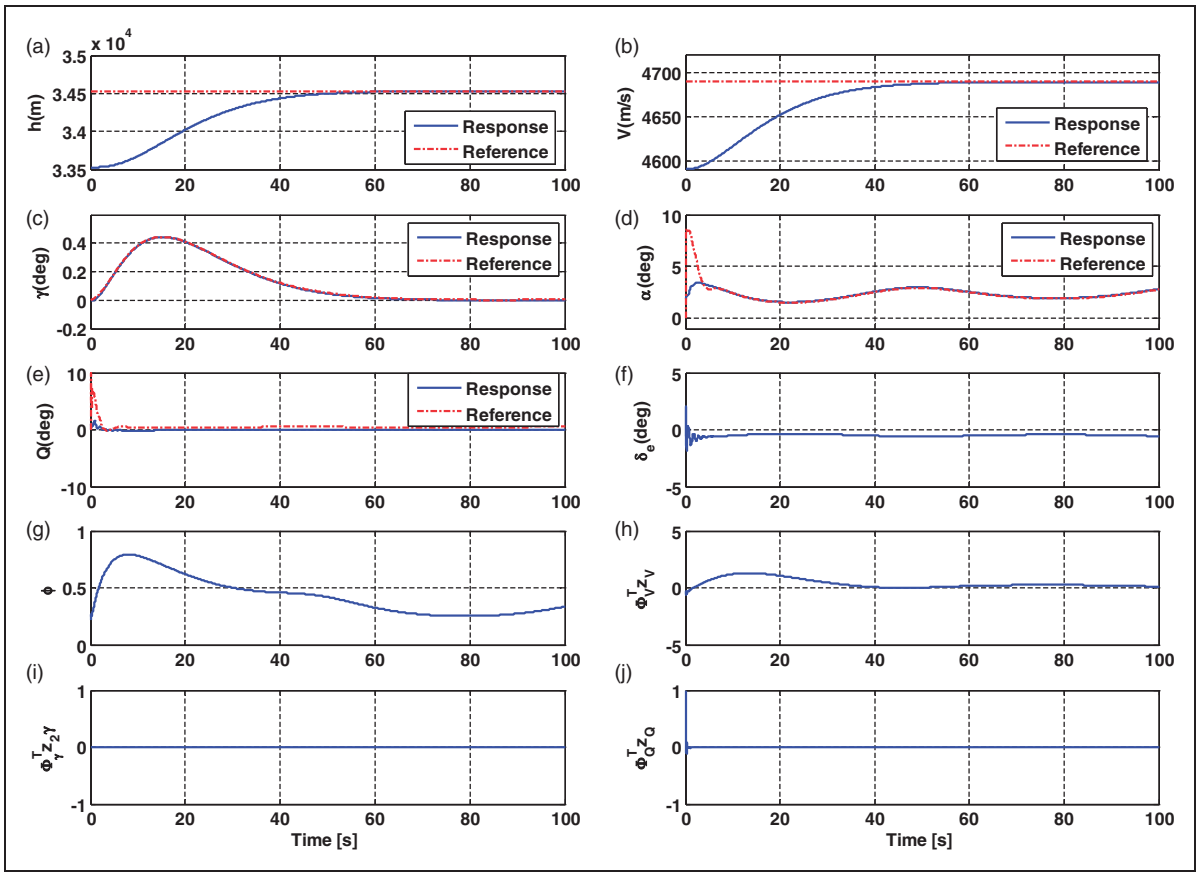

Figure 5. Responses to a 100 m/s step-velocity command and a 1000 m step-altitude command with parameter uncertainty.

The two kinds of reference trajectories discussed in the preceding simulation are used again. The simulation results are shown in Figures 5 and 6. Good tracking performances for the altitude, velocity, flight-path angle, angle of attack, and pitch rate in both cases can be seen in Figures 5(a) to (e) and 6(a) to (e), respectively. These states behave almost the same as those in the first set of simulations, except that the angle of attack oscillates slightly. Figures 5(f) and (g) and 6(f) and (g) show the deflections of the elevator δ_e and the fuel equivalence ratio ϕ. They all behave within their physical bounds in each case, which is also the same as in the first set of simulations. However, compared with those in the first set of simulations, the actuators oscillate slightly to handle the parameter uncertainty. $\boldsymbol{\Phi}_V(\cdot)^T z_V$, $\Phi_\gamma(\cdot) z_{2\gamma}$, and $\boldsymbol{\Phi}_Q(\cdot)^T z_Q$ in Figures 5(h) to (j) and 6(h) to (j) still converge to zero, which implies the convergence of the compensated tracking errors. It can be seen that the proposed control system provides good performance despite the presence of parameter uncertainty, which illustrates the robustness of this scheme.

Simulation for comparison

For comparison, a controller designed using the incorporation of pole placement and feedback linearization[44] is simulated for the same conditions as in the prior simulations. To guarantee a fair and meaningful comparison between this method and the proposed one, the controller parameters in this method are tuned to obtain a similar tracking performance of the altitude and velocity commands as the proposed one.[42] The results are shown in Figures 7 to 9. Figures 7(a), (c), (e), (g), and (i); 8(a) and (c); and 9(a) and (c) are the results evaluated on the nominal model, while the rest are the results evaluated on the model with parameter uncertainty discussed in the second set of simulations. For the first kind of reference trajectory, despite a similar tracking performance of the altitude and velocity commands, the attitude angles change severely as shown in Figure 7, which is disadvantageous to scramjet engines. This problem becomes worse for the actuators as shown in Figure 8, especially when there exists parameter uncertainty as shown in Figure 8(b) and (d), which is energy wasting and harmful for the structure of the actuators. Figure 9 shows the responses to a 200 m/s step-velocity command and a square wave-altitude command using this method. The simulations are enforced to stop within 80 s because the velocity decreases to the minimum value allowed for a cruise HSV.[24] It cannot deal with this kind of maneuvers using a

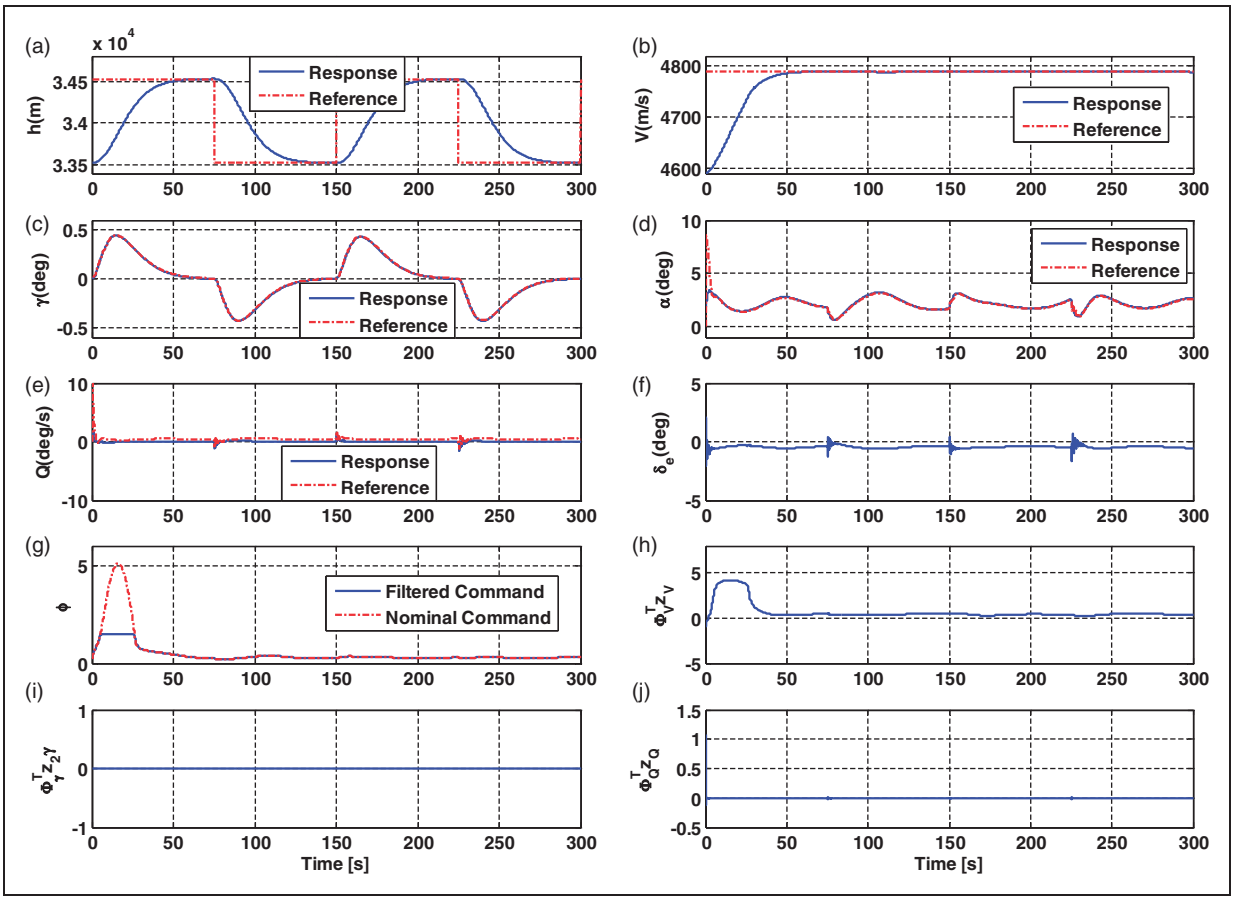

Figure 6. Responses to a 200 m/s step-velocity command and a square wave-altitude command with parameter uncertainty.

parameter-fixed controller, thus gain scheduling is needed. Combining the three sets of simulations, it clearly demonstrates the superiority of the proposed nonlinear adaptive control system.

Conclusions

A new scheme of nonlinear adaptive control system based on the I&I method is designed for the longitudinal HSV dynamics with all the aerodynamic

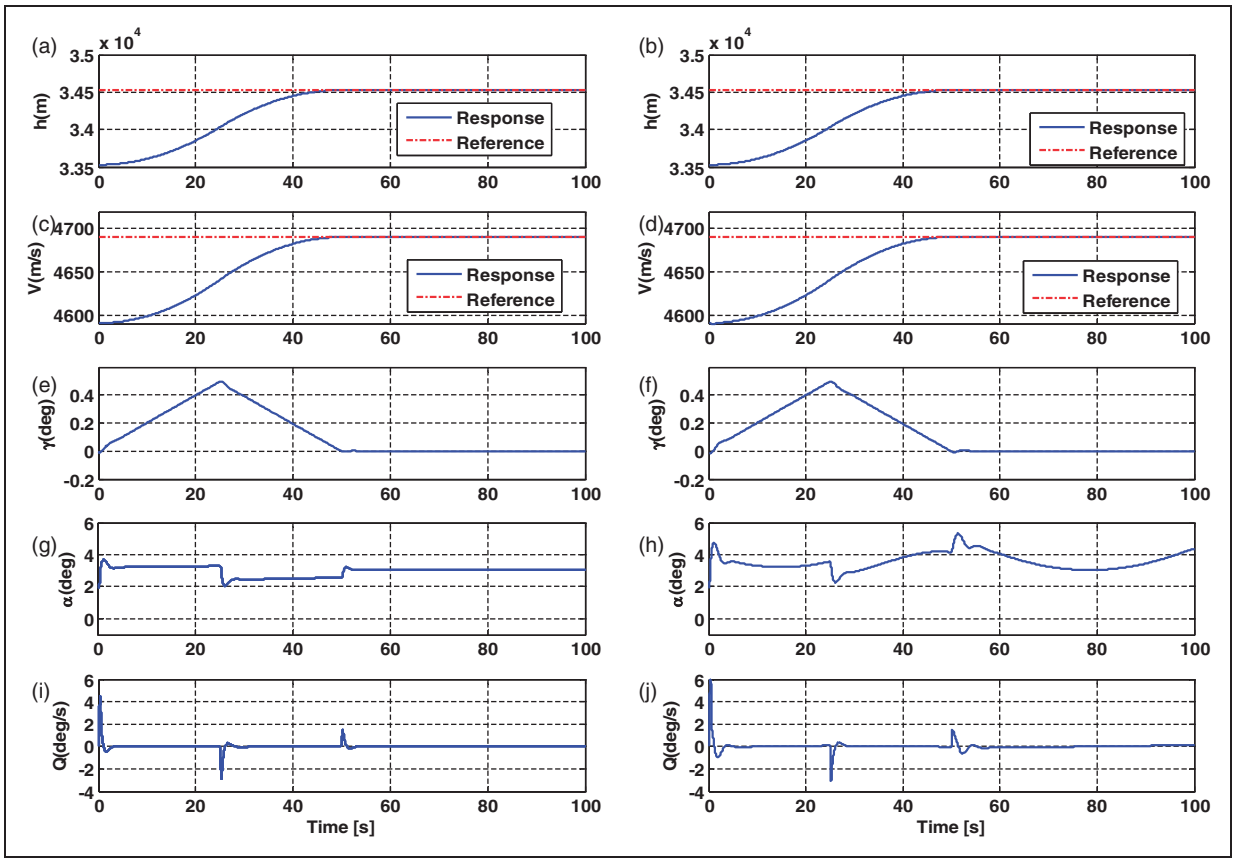

Figure 7. Responses to a 100 m/s step-velocity command and a 1000 m step-altitude command using the incorporation of pole placement and feedback linearization.

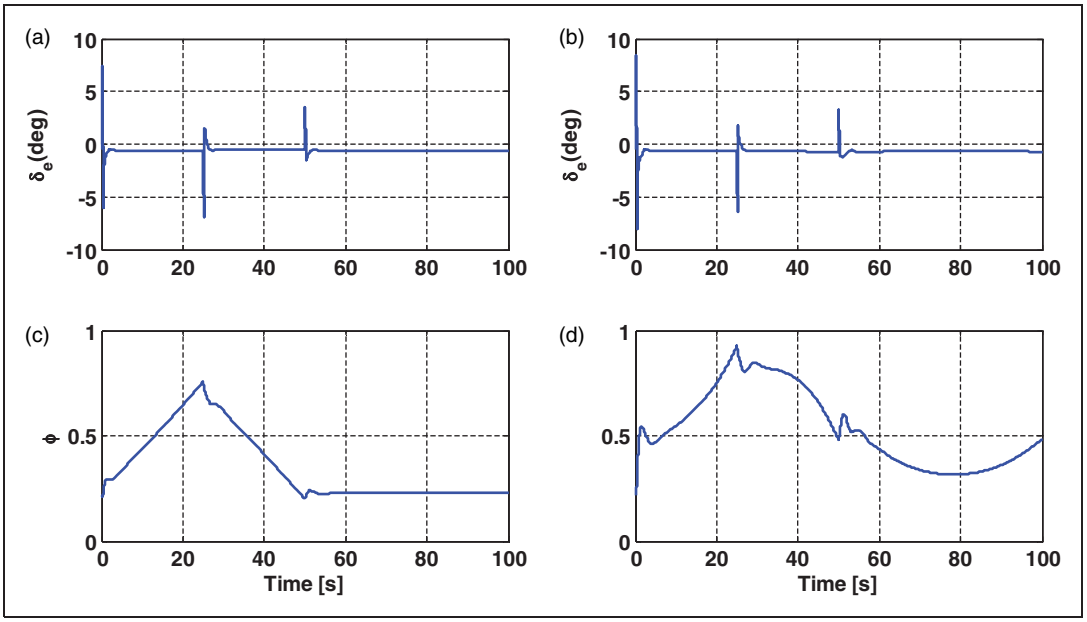

Figure 8. Actuator responses to a 100 m/s step-velocity command and a 1000 m step-altitude command using the incorporation of pole placement and feedback linearization.

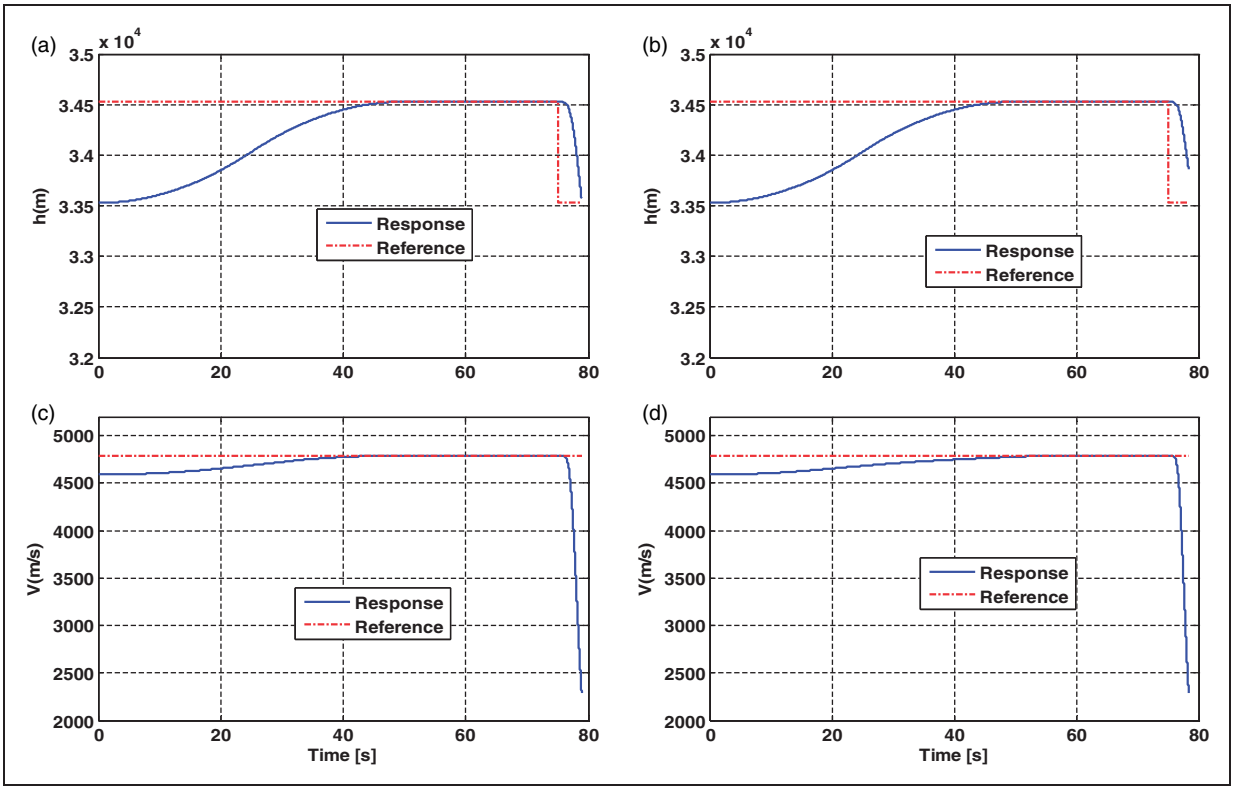

Figure 9. Responses to a 200 m/s step-velocity command and a square wave-altitude command using the incorporation of pole placement and feedback linearization.

parameters unknown in this paper. The architecture of the whole control system is constructed by decomposing the longitudinal dynamics into the velocity, altitude/flight-path angle, and angle of attack/pitch rate subsystems and using a constrained backstepping procedure. An I&I based controller, which is capable of achieving expected performance in spite of parameter uncertainties, is designed for each subsystem. This method provides a non-certainty-equivalent control system consisting of a control module and a separately designed parameter estimator. Command filters are used to prevent the state and actuator constraints from corrupting the parameter update laws. Simultaneously, globally asymptotic stability of the whole closed-loop system is derived by Lyapunov functions. It must be emphasized that the control scheme proposed here is much easier to tune than the one from Lyapunov-based methods, since one can assign appointed stable dynamics to the parameter estimate errors.

Representative simulations are performed. The results show great effectiveness of the proposed nonlinear adaptive control system, under the condition where all the aerodynamic coefficients are treated as unknown parameters. It should be noted that the proposed approach can also handle other uncertainties.

Funding

This study was supported by the National Natural Science Foundation of China (grant numbers 61273149, 61203003, 61273336) and the Innovation Method Fund of China (grant number 2012IM010200).

Conflict of interest

None declared.

References

1. Fidan B, Mirmirani M, and Ioannou P. Flight dynamics and control of air-breathing hypersonic vehicles: review and new directions. In: *Proceedings of 12th AIAA international space planes and hypersonic systems and technologies*, Norfolk, VA, 15–19 December 2003, AIAA paper no. 2003–7081, pp.1–38. Virginia: AIAA.
2. Michael AB. An overview on dynamics and controls modeling of hypersonic vehicles. In: *Proceedings of American control conference,* St. Louis, MO, 10–12 June 2009, pp.2507–2512. New Jersey: IEEE.
3. Kuipers M, Mirmirani M, Ioannou P, et al. Adaptive control of an aeroelastic airbreathing hypersonic crusie vehicle. In: *Proceedings of AIAA guidance, navigation and control conference and exhibit*, Hilton Head, South Carolina, 20–23 August 2007. AIAA paper no. 2007–6326, pp.1–12. Virginia: AIAA.
4. Buschek H and Calise AJ. Uncertainty modeling and fixed-order controller design for a hypersonic vehicle model. *J Guid Control Dynam* 1997; 20: 42–48.
5. Sigthorsson DO, Jankovsky P, Serrani A, et al. Robust linear output feedback control of an airbreathing hypersonic vehicle. *J Guid Control Dynam* 2008; 31: 1052–1066.
6. Gibson TE, Crespo LG and Annaswamy AM. Adaptive control of hypersonic vehicles in the presence of

modeling uncertainties. In: *Proceedings of American control conference*, St. Louis, MO, 10–12 June 2009, pp.3178–3183. New Jersey: IEEE.
7. Ioannou PA and Sun J. *Robust adaptive control*. New York: Dover Publication, 1996, pp.7–8.
8. Xu HJ, Mirmirani M and Ioannou P. Adaptive sliding mode control design for a hypersonic flight vehicle. *J Guid Control Dynam* 2004; 27: 829–838.
9. Liu YB and Lu YP. Nonlinear fuzzy robust adaptive control of a longitudinal hypersonic aircraft model. In: *Proceedings of international conference on artificial intelligence and computational intelligence*, Shanghai, China, 7–8 November 2009, pp.31–35. New Jersey: IEEE.
10. Parker JT, Serrani A, Yurkovich S, et al. Approximate feedback linearization of an air-breathing hypersonic vehicle. In: *Proceedings of AIAA guidance, navigation and control conference and exhibit*, Keystone, Colorado, 21–24 August 2006, AIAA paper no. 2006–6556, pp.1–16. Virginia: AIAA.
11. Parker JT, Serrani A, Yurkovich S, et al. Control-oriented modeling of an air-breathing hypersonic vehicle. *J Guid Control Dynam* 2007; 30: 856–869.
12. Rehman OU, Fidan B and Petersen IR. Robust minimax optimal control of nonlinear uncertain systems using feedback linearization with application to hypersonic flight vehicles. In: *Proceedings of 48th IEEE conference on decision and control and 28th Chinese control conference*, Shanghai, China, 15–18 December 2009, pp.720–726. New Jersey: IEEE.
13. Sun HB, Li SH and Sun CY. Finite time integral sliding mode control of hypersonic vehicles. *Nonlinear Dynam* 2013; 73: 229–244.
14. Zong Q, Wang J, Tian BL, et al. Quasi-continuous high-order sliding mode controller and observer design for flexible hypersonic vehicle. *Aerosp Sci Technol* 2013; 27: 127–137.
15. Hu XX, Wu LG, Hu CH, et al. Adaptive sliding mode tracking control for a flexible air-breathing hypersonic vehicle. *J Franklin Inst* 2012; 349: 559–577.
16. Li HB, Sun ZQ, Min HB, et al. Fuzzy dynamic characteristic modeling and adaptive control of nonlinear systems and its application to hypersonic vehicles. *Sci China (Inf Sci)* 2011; 54: 460–468.
17. Lian CB, Shi LB, Ren Z, et al. Fuzzy sliding mode variable structure controller for hypersonic cruise vehicle. In: T Xiao, L Zhang and S Ma (eds) *ICSC 2012, Part I, CCIS 326*. Heidelberg, Berlin: Springer, 2012, pp.137–146.
18. Wang YF, Jiang CS and Wu QX. Attitude tracking control for variable structure near space vehicles based on switched nonlinear systems. *Chinese J Aeronaut* 2013; 26: 186–193.
19. Xu HJ, Mirmirani M and Ioannou P. Robust neural adaptive control of a hypersonic aircraft. In: *Proceedings of AIAA guidance, navigation and control conference and exhibit*, Austin, Texas, 11–14 August 2003, AIAA paper no. 2003–5641, pp.1–8. Virginia: AIAA.
20. Xu B, Wang DW, Sun FC, et al. Direct neural discrete control of hypersonic flight vehicle. *Nonlinear Dynam* 2012; 70: 269–278.
21. Sonneveldt L, Chu QP and Mulder JA. Nonlinear flight control design using constrained adaptive backstepping. *J Guid Control Dynam* 2007; 30: 322–336.
22. Kanellakopoulos I, Kokotovic P and Morse A. Systematic design of adaptive controllers for feedback linearizable systems. *IEEE Trans Autom Control* 1991; 36: 1241–1253.
23. Xu B, Sun FC, Yang CG, et al. Adaptive discrete-time controller design with neural network for hypersonic flight vehicle via back-stepping. *Int J Control* 2011; 84: 1543–1552.
24. Fiorentini L, Serrani A, Bolender MA, et al. Nonlinear robust adaptive control of flexible air-breathing hypersonic vehicles. *J Guid Control Dynam* 2009; 32: 401–416.
25. Poulain F, Piet-Lahanier H and Serre L. Nonlinear control of an airbreathing hypersonic vehicle: A backstepping approach. *Autom Control Aerosp* 2010; 1: 1–6.
26. Ji YH, Zong Q and Zeng F. Immersion and invariance based nonlinear adaptive control of hypersonic vehicles. In: *Proceedings of 24th Chinese control and decision conference*, Taiyuan, China, 23–25 May 2012, pp.2025–2030. New Jersey: IEEE.
27. Li SH, Sun HB and Sun CY. Composite controller design for an airbreathing hypersonic vehicle. *Proc IMechE, Part I: J Systems and Control Engineering* 2012; 226: 651–664.
28. Yang J, Li SH, Sun CY, et al. Nonlinear-disturbance-observer-based robust flight control for airbreathing hypersonic vehicles. *IEEE Trans Aerosp Electron Syst* 2013; 49: 1263–1275.
29. Astolfi A and Ortega R. Immersion and invariance: A new tool for stabilization and adaptive control of nonlinear systems. *IEEE Trans Autom Control* 2003; 48: 590–606.
30. Astolfi A, Karagiannis D and Ortega R. *Nonlinear and adaptive control with applications*. London: Springer-Verlag, 2008Chaps. 2, 4.
31. Karagiannis D and Astolfi A. Non-linear and adaptive flight control of autonomous aircraft using invariant manifolds. *Proc IMechE, Part G: J Aerospace Engineering* 2010; 224: 403–415.
32. Zhang JM, Li Q, Cheng N, et al. Adaptive dynamic surface control for unmanned aerial vehicles based on attractive manifolds. *J Guid Control Dynam* 2013; 36: 1776–1783.
33. Kobayashi Y and Takahashi M. Design of nonlinear adaptive flight control system based on immersion and invariance. In: *Proceedings of AIAA guidance, navigation, and control conference*, Chicago, Illinois, 10–13 August 2009, AIAA paper no. 2009–6174, pp.1–20. Virginia: AIAA.
34. Lee KW and Singh SN. Noncertainty-equivalent adaptive missile control via immersion and invariance. *J Guid Control Dynam* 2010; 33: 655–665.
35. Lee KW and Singh SN. Immersion- and invariance-based adaptive missile control using filtered signals. *Proc IMechE, Part G: J Aerospace Engineering* 2012; 226: 646–663.
36. Sonneveldt L, Van Oort ER, Chu QP, et al. Immersion and invariance based nonlinear adaptive flight control. In: *Proceedings of AIAA guidance, navigation, and control conference*, Toronto, Ontario, Canada, 2–5 August 2010, AIAA paper no. 2010–7690, pp.1–18. Virginia: AIAA.
37. Hu JC and Zhang HH. Immersion and invariance based command-filtered adaptive backstepping control of VTOL vehicles. *Automatica* 2013; 49: 2160–2167.

38. Trevor W, Michael AB, David BD, et al. An aerothermal flexible mode analysis of a hypersonic vehicle. In: *Proceedings of AIAA guidance, navigation and control conference and exhibit*, Keystone, Colorado, 21–24 August 2006, AIAA paper no. 2006–6647, pp.1–22. Virginia: AIAA.
39. Farrell J, Polycarpou M and Sharma M. On-line approximation based control of uncertain nonlinear systems with magnitude, rate and bandwidth constraints on the states and actuators. In: *Proceedings of the 2004 American control conference*, Boston, Massachusetts, 30 June–2 July 2004, pp.2557–2562. New Jersey: IEEE.
40. Farrell J, Sharma M and Polycarpou M. Backstepping-based flight control with adaptive function approximation. *J Guid Control Dynam* 2005; 28: 1089–1102.
41. Fiorentini L and Serrani A. Adaptive restricted trajectory tracking for a non-minimum phase hypersonic vehicle model. *Automatica* 2012; 48: 1248–1261.
42. Seo D and Akello MR. High-performance spacecraft adaptive attitude-tracking control through attracting-manifold design. *J Guid Control Dynam* 2008; 31: 884–891.
43. Hassan KK. *Nonlinear system*. 3rd ed. New Jersey: Prentice Hall, 2002, p.323.
44. Pu ZQ, Tan XM, Yi JQ, et al. Advanced inversion control for a hypersonic vehicle based on PSO and arranged transient process. In: *Proceedings of international conference on mechatronics and automation*, Beijing, China, 7–10 August 2011, pp.359–364. New Jersey: IEEE.

Appendix 1

Notation

$\bar{c}$	mean aerodynamic chord (m)
C_i	aerodynamic coefficients
D	drag (N)
h	altitude (m)
h_c	altitude reference trajectory (m)
I_{yy}	moment of inertia (kg m^2)
k_i	controller gains
L	lift (N)
m	vehicle mass (kg)
M	pitching moment (N m)
q	dynamic pressure (kg/(m s^2))
Q	pitch rate (rad/s)
Q_c	actual command trajectory for pitch rate (rad/s)
Q_{cd}	nominal command trajectory for pitch rate (rad/s)
r	radial distance from Earth's center (m)
$r_{iV}, r_{i\gamma}, r_{iQ}$	parameters of update law
R_E	radius of the Earth (m)
S	reference area (m^2)
T	thrust (N)
V	velocity (m/s)
V_c	velocity reference trajectory (m/s)
z_i	parameter errors
α	angle of attack (rad)
α_c	actual command trajectory for angle of attack (rad)
α_{cd}	nominal command trajectory for angle of attack (rad)
$\beta_{iV}, \beta_{i\dot{\gamma}}, \beta_{iQ}$	nonlinear functions used in parameter estimators
γ	flight-path angle (rad)
γ_c	actual command trajectory for flight-path angle (rad)
γ_{cd}	nominal command trajectory for flight-path angle (rad)
δ_e	elevator deflection (rad)
δ_{e_c}	actual command for elevator deflection (rad)
δ_{e_cd}	nominal command for elevator deflection (rad)
θ_i	unknown parameters
$\hat{\theta}_i$	partial estimates of the unknown parameters
μ	gravitational constant
$\tilde{\bullet}$	tracking error, for example, $\tilde{h} = h - h_c$
ϕ	fuel equivalence ratio
ϕ_c	actual command for fuel equivalence ratio
ϕ_{cd}	nominal command for fuel equivalence ratio